Temperature Dependence of and Ligation Effects on Long-Range Electron Transfer in Complementary [Zn,Fe^{III}]Hemoglobin Hybrids

Sydney E. Peterson-Kennedy,[1a] Jacqueline L. McGourty,[1b] Juliette A. Kalweit, and Brian M. Hoffman*

Contribution from the Departments of Chemistry and Biochemistry and Molecular Biology and Cell Biology, Northwestern University, Evanston, Illinois 60201. *Received August 15, 1985*

Abstract: This report presents the first full temperature response of long-range electron transfer within a protein electron-transfer complex of known architecture, the [Zn,Fe^{III}]hemoglobin hybrids. For both hybrids k_t exhibits a thermally activated regime in which nonadiabatic electron transfer is coupled to thermal vibrations and/or fluctuations within the α_1-β_2 electron-transfer complex and its environment. Below ca. 160 K, k_t is independent of temperature and the transfer process occurs by nonadiabatic electron tunneling in which the accompanying nuclear rearrangement proceeds by nuclear tunneling. The transition between these two regimes differs in the two hybrids because of different responses of the ferriheme (Fe^{III}P) coordination state to cooling. Variable-temperature optical measurements and EPR spectroscopy show that the H_2O heme ligand of the [α(Fe$^{III}H_2O$),β(Zn)] species is replaced by the imidazole of the distal histidine upon cooling, but the heme ligation of the [α(Zn),β(Fe$^{III}H_2O$)] hybrid remains invariant. Analysis of the data in terms of the quantum-mechanical theory of vibronically coupled electron tunneling permits us to make comparisons with results for electron transfer in ruthenium-modified proteins, as well as with electron transfer from the cytochrome-to-bacteriochlorophyll special pair in the photosynthetic reaction center of *C. vinosum*.

We have shown recently that long-range electron transfer[2,3] between redox centers rigidly held at fixed and known distance and orientation can be studied by substituting zinc protoporphyrin for heme in one of the partners of a protein electron-transfer *complex*.[4-6] Mixed-metal [Zn,Fe][7] hybrid hemoglobins[8] represent the most fully characterized system employed and provide an ideal model for the study of electron transfer because the locations of all atoms involved in the electron-transfer process are crystallographically known to high precision.[9,10] Chains of one type (α or β) are substituted with closed-shell zinc protoporphyrin IX (ZnP) and chains of the opposite type are oxidized to the ferriheme (Fe^{III}P) state. In the deoxyhemoglobin structure[9] adopted by these hybrids,[8b,10] the prosthetic groups of closest approach are α_1^{Fe}-β_2^{Zn} (or the reverse substitution), and for present purposes we treat the molecule as two independent electron-transfer complexes, each composed of an α_1-β_2 subunit pair.[4a] The redox centers are separated by two heme pocket walls, one from each chain, at a metal-metal distance of 25 Å.[9] The ZnP and FeP planes are roughly parallel, and the shortest distance between atoms of the rings is ca. 20 Å.

Reversible electron transfer within a zinc-substituted protein electron-transfer complex is initiated by flash photoproduction of the slowly decaying zinc protoporphyrin triplet state (^{3}ZnP). The ^{3}ZnP is a good reductant[11] and can reduce its ferriheme partner by long-range electron transfer

$$^3\text{ZnP} + \text{Fe}^{III}\text{P} \xrightarrow{k_t} \text{ZnP}^{+} + \text{Fe}^{II}\text{P};\ \Delta E_0' \sim 0.8\ \text{V} \quad (1)$$

thereby forming an intermediate that returns to the ground state by back electron transfer from Fe^{II}P to the cation radical, ZnP^{+},

$$\text{ZnP}^{+} + \text{Fe}^{II}\text{P} \xrightarrow{k_h} \text{ZnP} + \text{FeP};\ \Delta E_0' \sim 1.0\ \text{V} \quad (2)$$

In the [Zn,Fe] hybrids, $k_h \gg k_t$ and flash photolysis techniques allow us to measure k_t accurately but only give lower bounds to k_h.[4]

A key advantage of this approach is that it permits us to measure transfer rates over a wide range of temperatures because the electron-transfer process is photoinitiated and occurs unimolecularly. We recently reported preliminary measurements of the temperature variation of the electron-transfer rate, k_t, for the [α(Fe^{III}),β(Zn)] hybrid.[5] We now describe the full temperature dependence of this long-range transfer process in the two complementary hybrids, using both α(Zn) and β(Zn) substitutions. The present study represents the first full characterization of

(1) Present addresses: (a) Chemistry Department, Whitworth College, Spokane, WA; (b) Chemistry Department, University of California, Davis, CA.

(2) Excellent reviews: (a) DeVault, D. *Quantum-Mechanical Tunnelling in Biological Systems*; Cambridge University: New York, 1984. (b) Newton, M. D.; Sutin, N. *Annu. Rev. Phys. Chem.* **1984**, *35*, 437-480. (c) Marcus, R. A. In *Tunneling in Biological Systems*; Chance, B., et al., Eds.; Academic: New York, 1979, pp 109-127. (d) Marcus, R. A.; Sutin, N. *Biochim. Biophys. Acta* **1985**, *811*, 265-322.

(3) Examples of the work in this area paralleling our own include the following: (a) Kostic, N. M.; Margalit, R.; Che, C.-M.; Gray, H. B. *J. Am. Chem. Soc.* **1983**, *105*, 7765-7767. (b) Isied, S. S.; Kuehn, C.; Worosila, G. *J. Am. Chem. Soc.* **1984**, *106*, 1722-1726. (c) Simolo, K. P.; McLendon, G. L.; Mauk, M. R.; Mauk, A. G. *J. Am. Chem. Soc.* **1984**, *106*, 1722-1726. (d) Nocera, D. G.; Winkler, J. R.; Yocom, K. M.; Bordignon, E.; Gray, H. B. *J. Am. Chem. Soc.* **1984**, *106*, 5145-5150. (e) Cho, K. C.; Che, C. M.; Cheng, F. C.; Choy, C. L. *J. Am. Chem. Soc.* **1984**, *106*, 6843-6844. (f) Miller, J. R.; Calcaterra, L. T.; Closs, G. L. *J. Am. Chem. Soc.* **1984**, *106*, 3047-3049. (g) McLendon, G. L.; Winkler, J. R.; Nocera, D. G.; Mauk, M. R.; Mauk, A. G.; Gray, H. B. *J. Am. Chem. Soc.* **1985**, *107*, 739-740. (h) Isied, S. S.; Kuehn, C.; Worosila, G. *J. Am. Chem. Soc.* **1984**, *106*, 1722-1726. (i) Crutchley, R. J.; Ellis, W. R.; Gray, H. B. *J. Am. Chem. Soc.* **1985**, *107*, 5092-5094.

(4) (a) Peterson-Kennedy, S. E.; McGourty, J. L.; Ho, P. S.; Sutoris, C. J.; Liang, N.; Zemel, H.; Blough, N. V.; Margoliash, E.; Hoffman, B. M. *Coord. Chem. Rev.* **1985**, *64*, 125-133. (b) McGourty, J. L.; Blough, N. V.; Hoffman, B. M. *J. Am. Chem. Soc.* **1983**, *105*, 4470-4472.

(5) Peterson-Kennedy, S. E.; McGourty, J. L.; Hoffman, B. M. *J. Am. Chem. Soc.* **1984**, *106*, 5010-5012.

(6) Ho, P. S.; Sutoris, C.; Liang, N.; Margoliash, E.; Hoffman, B. M. *J. Am. Chem. Soc.* **1985**, *107*, 1070-1071.

(7) Abbreviations: Hb, hemoglobin; metHb, ferric Hb; P, protoporphyrin IX; ZnP,Zn^{II}P; [Zn,Fe], hemoglobin derivative in which the two chains of a single type, α or β, are substituted with ZnP. When the specific oxidation and/or ligation state is of importance, it is indicated, e.g., [Zn,Fe^{II}CO]. When a particular hybrid is discussed, it is so indicated, e.g., [α(Fe$^{III}H_2O$),β(Zn)].

(8) (a) Hoffman, B. M. *Porphyrins* **1979**, *7*, 403-444 and references therein. (b) Blough, N. V.; Zemel, H.; Hoffman, B. M.; Lee, T. C. K.; Gibson, Q. H. *J. Am. Chem. Soc.* **1980**, *102*, 5683-5685. (c) Leonard, J. J.; Yonetani, T.; Callis, J. B. *Biochemistry* **1974**, *13*, 1460-1464.

(9) (a) Dickerson, R. E.; Geis, I. *Hemoglobin: Structure, Function, Evolution, and Pathology*; Benjamin/Cummings: Menlo Park, CA, 1983. (b) Fermi, G.; Perutz, M. F. *Atlas of Molecular Structures in Biology: Haemoglobin and Myoglobin*; Phillips, D. C.; Richards, F. M., Eds.; Oxford University: 1981; Vol. 2.

(10) The crystal structure of the analogous hybrid [α(FeCO),β(Mn^{III})] has been determined: Arnone, A.; Rogers, P.; Blough, N. V.; McGourty, J. L.; Hoffman, B. M. *J. Mol. Biol.*, in press. Crystals of [α(Fe^{II}CO),β(Zn)] have been prepared and their structure likewise will be determined.

(11) (a) Work in progress indicates that $E_0'((\text{ZnP})^{+}) \approx +1.2$ V (NHE) for, $e^- + (\text{ZnHb})^{+} = \text{ZnHb}$. In addition we take $\Delta E_T = E(^3\text{ZnP}) - E(\text{ZnP}) = 1.84$ V (ref 11b) and $E_0'(\text{Hb}^{+}) = 0.15$ V (NHE, ref 11c) in the equations, $\Delta E_0'(1) = \Delta E_T - E_0'((\text{ZnP})^{+}) + E_0'(\text{Hb}^{+})$; $\Delta E_0'(2) = \Delta E_T - \Delta E_0'(1)$. (b) Stanford, M. A., and Hoffman, B. M. *J. Am. Chem. Soc.* **1981**, *103*, 4104-4114. (c) For example: Bull, C.; Hoffman, B. M. *Proc. Natl. Acad. Sci. U.S.A.* **1975**, *72*, 3382-3386.

0002-7863/86/1508-1739$01.50/0

nonadiabatic electron transfer in a system in which the molecular architecture is crystallographically known to high resolution. Analysis of the full temperature response in terms of the quantum-mechanical theory of vibronically coupled electron tunneling[12] permits us to make comparisons with studies of electron transfer at ca. 0 °C and above within ruthenium-modified proteins,[3a-c,h,i] as well as with the seminal study of electron transfer in the photosynthetic reaction center of *C. vinosum*.[2,13] The present measurements also provide an unexpected illustration of the sensitivity of the electron-transfer rate to the ligation state of the ferriheme electron acceptor. An anomaly in the temperature response of k_t for the [α(Fe^{III}),β(Zn)] hybrid is shown, by using optical and ESR spectroscopies, to arise from replacement of H_2O as the sixth ligand by the distal imidazole.

Experimental Section

Materials. Hemoglobin (Hb), acquired from Evanston Hospital, was purified, separated into chains that could be metal-substituted, and reassembled into hybrid tetramers, as described.[14,15] The Hb hybrids were stored in liquid N_2 as the stable[20] [Zn,Fe^{II}CO]Hb. KH_2PO_4 and K_2HPO_4·$3H_2O$ (analytical grade) were purchased from Mallinckrodt; glycerol (reagent grade) was available from Eastman; ethylene glycol and methylene blue were purchased from Matheson, Coleman & Bell; $K_3Fe(CN)_6$ was available from Allied Chemical; phytic acid (IHP), Sephadex (G-25-150), and imidazole (Grade III) were from Sigma; sodium dithionite and potassium fluoride were purchased from Fisher (the $Na_2S_2O_4$ was used fresh); potassium cyanide was purchased from Baker; prepurified nitrogen from Liquid Air Corp. was used for all degassing operations.

Hb Hybrid Oxidation. The protein in the oxidized state is less stable than that in the ligated (CO) reduced state; therefore, to avoid the need for storing oxidized hybrid for long periods of time (months), only small amounts were prepared at a time. An aliquot of reduced hybrid (~5 mg in 0.5 mL) was thawed at 0 °C and purged with N_2 for 30 min to remove CO. This sample was run through a small (3-mL) column of Sephadex G-25 equilibrated with 0.2 M phosphate (pH 7.0). A 1.5- to 5-fold molar excess[16] of 0.1 M $K_3Fe(CN)_6$ was added per Fe^{II} heme and the sample was purged with N_2 on ice until the oxidation was complete, <30 min. The reaction was monitored spectroscopically with a final absorbance ratio (absorbance at 406/absorbance at 422) of ~ 0.72 for the [α-($Fe^{III}H_2O$),β(Zn)] hybrid and a ratio of ~0.68 for the [α(Zn),β-($Fe^{III}H_2O$)] hybrid.[14] The sample was then run over two 3-mL Sephadex G-25 columns equilibrated with 0.2 M phosphate (pH 7.0) to remove ferrocyanide and excess ferricyanide and then passed over a 3-mL column equilibrated with 0.01 M phosphate (pH 7.0). To ensure removal of ferricyanide, which quenches the zinc porphyrin triplet state, a second 0.2 M phosphate column was run as a precaution. The oxidized Hb hybrids, [Zn,Fe^{III}], were then stored in liquid N_2. ZnP is light- and oxygen-sensitive; therefore, all preparations and measurements involving the zinc-substituted Hb hybrids were accomplished with as little light as possible.

Hb Hybrid Reduction. When desired, oxidized Hb hybrids were reduced by using a deaerated stock solution of sodium dithionite in 0.01 M phosphate (pH 8.0)[17] that had been standardized previously by titration with deaerated methylene blue (ϵ(661 nm) = 66.1 mM^{-1}).[18] A stoichiometric amount of the dithionite stock solution was added to the deaerated Hb hybrid sample under a positive pressure of N_2. The reduction was immediate, as observed spectroscopically.

Buffers. Cryosolvents[19] used included the following: (1) (ethylene glycol/0.05 M phosphate) (2/1 by volume), 10 μM IHP (pH 6.0); (2) (0.01 M phosphate/glycerol) (1/1 by volume), 10 μM IHP (pH 6.0); (3) 0.01 M phosphate (no cosolvent), 10 μM IHP (pH 7.0). Reported pH values were measured at room temperature. The cryosolvents were prepared with distilled water, K_2HPO_4 and KH_2PO_4 salts, and the desired cosolvent. Inosital hexaphosphate (IHP) was added in 1.25- to 5-fold excess per tetramer to ensure that the protein was locked in the T-state conformation.[8b,20] The cryosolvents were brought to a final pH of 6.0 and a selected concentration of cosolvent by the addition of a stock solution of IHP (0.01 M) and monobasic and dibasic phosphate stock solutions (0.01 M or 0.05 M) to the appropriate volume of cosolvent. Cosolvents were used without further purification. The ethylene glycol cryosolvent was used for data collection from 150 to 313 K; the glycerol cryosolvent was used for temperature ranges of 77 to 170 K and 250 to 313 K; the pH was chosen such that upon cooling to 198 K it was equal to 7.0.[19] Phosphate buffer without cosolvents was used from 273 to 313 K. In the overlapping temperature ranges the ^{3}ZnP decay rate constants were independent of the solvent for each of the Hb hybrids in both the oxidized and reduced states.

Sample Preparation. Samples whose kinetic properties were to be monitored by optical absorption were prepared in 4- × 10-mm rectangular glass cells that were attached to standard-tapered joints to fit our variable-temperature optical Dewar and were also equipped with high-vacuum Teflon Kontes valves to facilitate oxygen-free preparations. Buffers were bubbled for a minimum of 20 min in a glass 10-mL Erlenmeyer flask sealed with a septum; the stock solutions of the oxidized Hb hybrids were purged in a 0.5-mL cryotube sealed with a septum; low flows of N_2 gas were used to prevent evaporation of the solvent. An empty low-temperature cell was pumped and purged with N_2 for at least 30 min and 20 cycles. The buffer was then added to the cell, followed by addition of the protein. All liquid transfers were made with gas-tight syringes and a positive pressure of N_2 gas, and each addition was followed by multiple cycles (10–20) of slight evacuation and backflush of N_2; bubbling the protein was avoided because this causes denaturation. The concentrations of the samples for the optical work were 2 to 8 μM hybrid Hb tetramer.

The formation of ligated species was accomplished by the slow addition with gentle mixing of deaerated stock solutions of imidazole (1 M; adjusted to pH 6.4 with HCl), KF (10 M), and KCN (0.1 M). The stock solutions were bubbled (in the hood) with N_2 for a minimum of 15 min. In all cases ligation occurred to 95% or greater.

Before ligands were added or low-temperature kinetic data were collected, the optical spectrum of a deaerated sample was examined, and the ^{3}ZnP rate of decay was measured at room temperature to ensure that the sample was oxygen-free. Samples that were degraded, as observed spectroscopically, were discarded; since oxygen quenches the ^{3}ZnP state, thereby increasing its rate of decay, samples that had a high rate of ^{3}ZnP decay were gently purged and pumped 25 times, which usually successfully removed trace amounts of oxygen.

For data acquired for the [α($Fe^{III}H_2O$),β(Zn)] hybrid, 16 independent samples were used; for the [α(Zn),β($Fe^{III}H_2O$)] hybrid, data were gathered from 9 independent samples. This number of samples was necessary because the [α($Fe^{III}H_2O$),β(Zn)] hybrid is photoreduced[4,14] by multiple flashes (see below) and the [α(Zn),β($Fe^{III}H_2O$)] hybrid undergoes slow autoreduction at temperatures above 273 K.

Samples whose optical spectra were to be measured as a function of temperature were also prepared in the 4-mm rectangular glass cells, but without deaeration. These studies employed the ethylene glycol/phosphate buffer cryosolvent. Samples for EPR measurements were prepared in the ethylene glycol/phosphate buffer cryosolvent; they were ~0.2 mM Hb tetramer and were placed in 3-mm quartz tubes. Some samples were prepared by plunging the room-temperature EPR tube into liquid N_2. Others were slowly cooled by placing the EPR tube in the N_2 variable-temperature optical Dewar and decreasing the temperature at a rate of ~60 deg/h from ambient to 175 K (~2 h); then the sample was plunged into liquid N_2.

Measurements. The flash photolysis apparatus for measuring transient absorption changes has been described.[21] Transients associated with the ^{3}ZnP formation and decay were monitored at 415 nm, the [Fe^{III}Hb-Fe^{II}Hb] isosbestic point. The actinic sources used were either a Sunpak 611 photographic flash filtered with the appropriate colored glass (Corning 3-71) or an Electrophotonics dye laser (R6G) (emission at 590 ± 10 nm)[22] attenuated with neutral-density filters. With these sources it was possible to vary the fraction, f, of ZnP that had been excited to the triplet state over the full range, $0 \leq f \leq 1.0$. When there is more than one ^{3}ZnP per hemoglobin tetramer, the ^{3}ZnP undergo quenching by long-range *intra*molecular triplet-triplet energy transfer.[23] This process

(12) (a) Jortner, J. *J. Chem. Phys.* **1976**, *64*, 4860–4867. (b) Siders, P.; Marcus, R. A. *J. Am. Chem. Soc.* **1981**, *103*, 741–747.
(13) DeVault, D.; Chance, B. *Biophys. J.* **1966**, *6*, 825–847.
(14) (a) McGourty, J. L.; Hoffman, B. M., manuscript in preparation. (b) McGourty, J. L., Ph.D. Thesis, Northwestern University.
(15) The hybrid preparation, ref 14, follows the procedures of N. V. Blough, Ph.D. Thesis, Northwestern University, 1983.
(16) Antonini, E.; Brunori, M. *Hemoglobin and Myoglobin in Their Reactions with Ligands*; American Elsevier: New York, 1971.
(17) Lambeth, D. O.; Palmer, G. *J. Biol. Chem.* **1973**, *248*, 6095–6103.
(18) Conn, H. J. *Biological Stains*; Williams & Wilkins: Baltimore, 1961, p 95.
(19) (a) Douzou, P. In *Methods of Biochemical Analysis*; Glick, D.; Ed.; Wiley: New York, 1974; Vol. 22; pp 401–512. (b) Fink, A. L.; Geeves, M. A. In *Methods in Enzymology*; Purich, D. L., Ed.; Academic: New York, 1979; Vol. 63; pp 336–371.
(20) (a) Shulman, R. G.; Hopfield, J. J.; Ogawa, S. *Q. Rev. Biophys.* **1975**, *8*, 325–420. (b) Edelstein, S. J. *Annu. Rev. Biochem.* **1975**, *44*, 209–232.
(21) Stanford, M. A.; Swartz, J. C.; Phillips, T. E.; Hoffman, B. M. *J. Am. Chem. Soc.* **1980**, *102*, 4492–4499.
(22) Rose, E. J.; Hoffman, B. M. *J. Am. Chem. Soc.* **1983**, *105*, 2866–2873.

is eliminated when the fraction of photoexcited ^{3}ZnP is low, $f \leq 15\%$. Thus, unless otherwise stated, all the measurements reported here refer to this low-photolysis level in the absence of such energy-transfer processes.

Variable-temperature optical measurements were made in a Dewar with quartz windows whose temperature was controlled by a flow of cold N_2 gas obtained from boiling liquid N_2 (for temperatures between 77 and 290 K) or by a Haake bath with water and methanol (1:1 by volume) (for temperatures between 260 and 313 K). The temperature increased or decreased in 2- to 3-deg increments with an average rate of 45 deg/h. The temperature was measured by a copper/constantan thermocouple.

Continuous wavelength (CW) irradiation was done with an Oriel Corporation xenon–mercury arc lamp (200 W) screened with a water filter to remove IR radiation and a Melles Griot UV filter (0-52).

A single-beam diode array Hewlett-Packard 8451 spectrophotometer, with wavelength accuracy of ±2 nm, was used for obtaining optical spectra. The variable-temperature optical Dewar was employed for spectra taken at subambient temperatures. The temperature was decreased at a rate of ca. 60 deg/h. With the optical Dewar as a reference, all the spectra were zeroed at 700 nm and stored on disk. Plots of the optical spectra and graphs of the spectral data were generated by a Hewlett-Packard 85 computer on the Hewlett-Packard 7470A graphics plotter.

The temperature dependences of the electron-transfer rate constant were fit to theoretical expressions on an Apple IIe computer, using a general nonlinear-least-squares[24] program.

The EPR data was taken on a highly modified Varian E-4.

Results

The rate constant of ^{3}ZnP decay in the reduced Hb hybrids [Zn,Fe^{II}] at ambient temperature is $k_D \cong 55\ s^{-1}$. This is comparable to the rate constant of ^{3}ZnP decay in the fully zinc substituted Hb.[23] In contrast, under the same conditions, the rate constant of ^{3}ZnP decay in the oxidized Hb hybrids, [Zn,Fe^{III}H$_2$O], is $k_{obsd} \cong 155\ s^{-1}$.[3] We address elsewhere[14] in detail the full variety of processes that might account for this increase in the ^{3}ZnP decay rate constant. Firstly, studies of the concentration dependence show the quenching to be intramolecular. By examining a series of ligated Hb hybrids we showed that neither ^{3}ZnP-to-Fe^{III}P energy transfer nor spin quenching by the paramagnetic heme centers contributes to the increase in the ^{3}ZnP decay rate constant of an oxidized Hb hybrid. Instead, the decay of ^{3}ZnP within a [Zn,Fe]Hb hybrid is enhanced by long-range electron transfer according to eq 1. In all cases considered here the rate constant for the back transfer is high, $k_h \gtrsim 10^2 k_D, 10^2 k_t$. In this regime, the electron-transfer rate constant, k_t, is calculated as follows: (1) The intrinsic rate constant for triplet decay, k_D, is obtained by measuring the decay of the ^{3}ZnP in the reduced Hb hybrids, [Zn,Fe^{II}]; in these species the heme has been reduced in advance and electron transfer is abolished. (2) The rate constant, k_{obsd}, is measured for the decay of the ^{3}ZnP in the oxidized Hb hybrids, [Zn,Fe^{III}H$_2$O]. (3) The rate constant for the long-range reduction of the aquoferriheme by ^{3}ZnP is obtained by subtraction:

$$k_t = k_{obsd} - k_D \qquad (3)$$

For example, at ambient temperature, $k_{obsd} = 155 \pm 4\ s^{-1}$ and $k_D = 55 \pm 2\ s^{-1}$ for [α(Zn),β(Fe^{III}H$_2$O)], and thus electron transfer from the ^{3}ZnP to Fe^{III}(H$_2$O)P rigidly held within the hybrid at a metal-to-metal distance of 25 Å occurs with a rate constant, $k_t = 100 \pm 6\ s^{-1}$. This value remains invariant between pH 6 and 7.

In addition to the thermal electron-transfer process of eq 2, there is an alternate decay channel, k_m, for the [ZnP$^+$,Fe^{II}P] intermediate, one in which (ZnP)$^+$ is reduced by an as-yet unidentified residue, thus leading to a net accumulation of Fe^{II}P.[14] Because the hybrids are characterized by the limit, $k_h, k_m \gg k_t$, the rate constants k_h, k_m cannot be measured accurately. Nevertheless, the quantum yield for the process by which decay of the intermediate leads to accumulation of reduced heme was determined at ambient temperature: $\phi_m = k_m/(k_h + k_m) = 0.37$. Considering

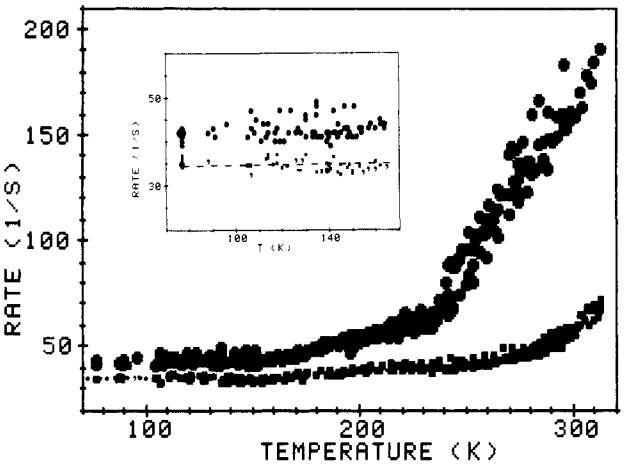

Figure 1. Temperature dependence of ^{3}ZnP decay rates in [α(Zn),β(Fe^{II})], k_D (■), and [α(Zn),β(Fe^{III}H$_2$O)], k_{obsd} (●). The curve represents the fit of k_D to eq 4; $C_1 = 34\ s^{-1}$; $C_2 = 6.0 \times 10^3\ s^{-1}$; $C_3 = -20\ s^{-1}\ K^{-1}$; $C_4 = 9.4 \times 10^{-1}\ s^{-1}\ K^{-1}$; $C_5 = 3.5 \times 10^{-4}\ s^{-1}\ K^{-3}$; $C_6 = 1.2 \times 10^{-3}$ K. Inset: Expanded view of data in temperature-independent regime. Curve as in main figure. The averages to k_D (77) and k_{obsd} (77) also are indicated as large (●) because of the numerous overlapping points.

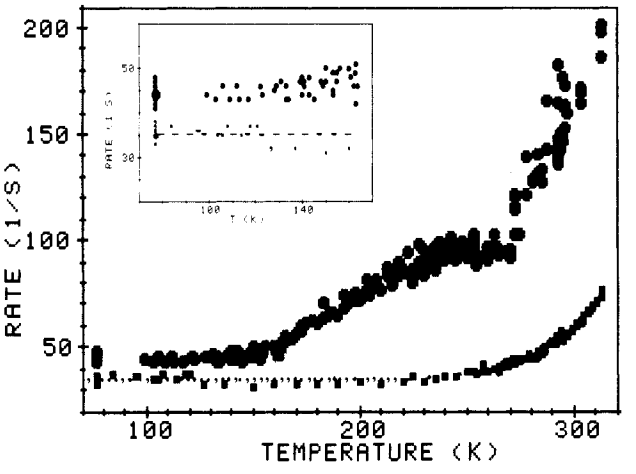

Figure 2. Temperature dependence of ^{3}ZnP decay rates in [α(Fe^{II}),β(Zn)], k_D (■), and [α(Fe^{III}),β(Zn)], k_{obsd} (●). The curve represents the fit of k_D to eq 4: $C_1 = 35\ s^{-1}$; $C_2 = 40 \times 10^3\ s^{-1}$; $C_3 = -21\ s^{-1}\ K^{-1}$; $C_4 = -8.2 \times 10^{-2}\ s^{-1}\ K^{-2}$; $C_5 = 4.3 \times 10^{-4}\ s^{-1}\ K^{-3}$; $C_6 = 1.3 \times 10^3$ K. Inset: Expanded view of data in temperature-independent regime. Curve as in main figure. The averages to k_D (77) and k_{obsd} (77) are indicated (●) as in Figure 1.

that the quantum yield for electron transfer from the ^{3}ZnP excited state is $\phi_t = k_t/(k_t + k_D) = 2/3$, the net quantum yield for heme photoreduction, based on ^{3}ZnP production, is $\phi_r = \phi_t\phi_m = 1/4$.

The observation of irreversible reduction has two consequences. Firstly, it unambiguously confirms that the ^{3}ZnP in the [Zn,Fe^{III}]Hb hybrids is quenched by electron transfer. Therefore, in order to obtain direct evidence for electron transfer at low temperatures, the [Zn,Fe^{III}]Hb hybrids were examined at 77 K. Ferroheme accumulation was not observed during multiple flash excitation cycles ($\sim$10). This is not surprising, since the quantum yield for electron transfer, ϕ_t, is reduced at 77 K (see below), and the same appears to be true for ferroheme production, ϕ_m.[14] Nevertheless, irreversible ferroheme formation is seen upon CW irradiation at 77 K. This observation directly demonstrates electron transfer in Hb hybrids at 77 K.[25]

Secondly, however, progressive reduction of the ferriheme site decreases the concentration of the ferriheme and thereby alters the ^{3}ZnP decay kinetics. Thus, all the data reported here was taken under "first flash" conditions, with fewer than 15% of the

(23) Zemel, H.; Hoffman, B. M. *J. Am. Chem. Soc.* **1981**, *103*, 1192–1201.

(24) Bevington, P. R. *Data Reduction and Error Analysis for the Physical Sciences*; McGraw-Hill: New York, 1969, pp 134–186.

(25) Because the samples existed as glasses with variable amounts of cracking, quantitative actinometry was not deemed feasible.

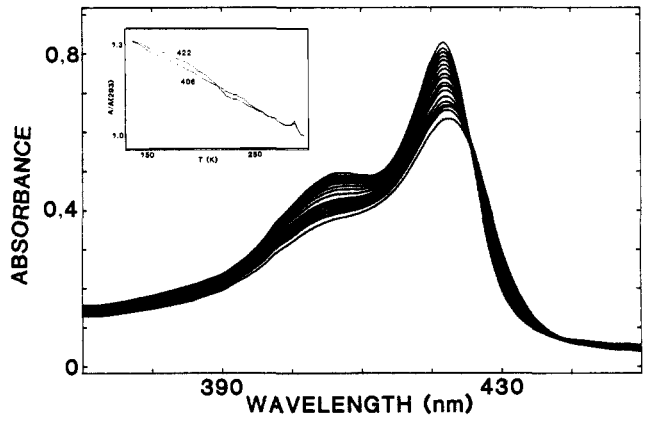

Figure 3. Temperature dependence of the optical spectrum of [α(Zn),-β($Fe^{III}H_2O$)]; T = 293–143 K (~10-deg increments). Inset: The values of the absorbances at 406 nm (the metHb Soret peak) and 422 nm (the ZnHb Soret peak), (~3-deg increments), each normalized to its value at ambient temperatures. Conditions: ethylene glycol/phosphate buffer cryosolvent; room temperature pH = 6.

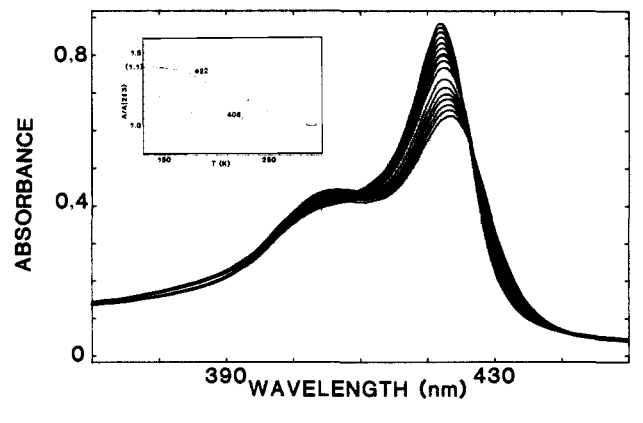

Figure 4. Temperature dependence of the optical spectrum of [α-(Fe^{III}),β(Zn)]; T = 293–143 K (~10-deg increments). The Soret bands do *not* smoothly increase in absorbance, due to the formation of bis(imidazole)hemichrome. Inset: The value of the absorbance at 406 nm (the metHb Soret peak) and at 422 nm (the ZnHb Soret peak) (~3-deg increments), each normalized to its value at ambient temperature. The curve for metHb is plotted on a different scale, indicated by parentheses. Conditions: ethylene glycol phosphate buffer cryosolvent; room temperature pH = 6.

hybrid hemes present in the reduced form, as determined spectroscopically.

Temperature Dependence of k_D. The intrinsic rate constant for ^{3}ZnP decay has been measured from 77 to 313 K in both [α(Zn),β(Fe^{II})] and [α(Fe^{II}),β(Zn)]Hb hybrids (Figures 1 and 2). The data for the [α(Zn),β(Fe^{II})] hybrid represent eight samples and a total of 240 kinetic determinations. For the [α-(Fe^{II}),β(Zn)] hybrid, 130 measurements were made on seven samples. Individual points in the figures may represent as many as seven overlapping measurements.

The ^{3}ZnP decay rate constants for the two reduced hybrids are almost indistinguishable; k_D decreases smoothly with decreasing temperature down to $T \sim 200$ K, and then remains constant upon further cooling. The data for the two hybrids has been fit to the function[26]

$$k_D = C_1 + (C_2 + C_3T + C_4T^2 + C_5T^3)(\exp(-C_6/T)) \quad (4)$$

solely in order to interpolate k_D as a function of temperature for eq 3; the parameters for the fits are given in the captions to Figures 1 and 2. The fits are excellent at all temperatures; conveniently, $k_D = C_1$ for $T \lesssim 200$ K.

Temperature Dependence of k_{obsd}. The temperature dependence of the rate constant for ^{3}ZnP decay in the [Zn,$Fe^{III}(H_2O)$] hybrids is presented in Figures 1 and 2. The data for the [α(Zn),β-($Fe^{III}H_2O$)] hybrid represent data taken on 10 samples and 290 kinetic measurements. For the [α(Fe^{III}),β(Zn)] hybrid, 170 measurements were made on 17 samples. For [α(Zn),β-($Fe^{III}H_2O$)] hybrid, k_{obsd} decreases smoothly as the temperature decreases from ambient to ~160 K, below which the rate constant is invariant down to 77 K. As reported earlier,[5] for the [α-($Fe^{III}H_2O$),β(Zn)] hybrid, k_{obsd} decreases smoothly from 313 to 250 K and is temperature-independent from ~170 K down to 77 K. At that time we were unable to make measurements between 170 and 250 K because in this range the glycerol/phosphate buffer cryosolvent devitrified and shattered the optical cell. Now, using the ethylene glycol/phosphate buffer cryosolvent, we have measured the ^{3}ZnP decay rate constant for this hybrid over the entire temperature range, 77–313 K. The results agree at temperatures where data have been taken with both cryosolvents. To our surprise we now find an anomaly in the temperature dependence of k_{obsd} in the hitherto unexplored range of 170–250 K, namely, a plateau in the range from 230 to 270 K (Figure 2). This anomaly is addressed in the following section.

Temperature Dependence of Optical Spectra. In order to ascertain the cause of the anomaly in the temperature variation of the triplet decay rate for the [α($Fe^{III}H_2O$),β(Zn)] hybrid, we examined the temperature dependence of the absorption spectra of the Hb hybrids (Figures 3 and 4). The spectrum of a hemoglobin chain containing a ZnP, in particular of ZnHb, is quite distinct from that of an $Fe^{III}(H_2O)$P chain or of aquometHb; the Soret maximum for ZnHb is 422 nm,[23] whereas that for the aquometHb and isolated subunits is 406 nm.[16] Thus, the peak at 422 nm in the spectra of the hybrids is representative of the ZnP-containing chain, the shoulder (peak) at 406 nm is representative of the $Fe^{III}(H_2O)$P chain, and one can monitor a particular type of chain within a hybrid by monitoring the appropriate wavelength. In order to display these trends, the absorbances at the wavelengths characteristic of the ZnP Soret band (λ = 422 nm) and of the $Fe^{III}(H_2O)$P Soret band (λ = 406 nm) were normalized to their respective values at 293 K and plotted as a function of temperature (Figures 3 and 4, insets).

When the temperature of the [α(Zn),β($Fe^{III}(H_2O)$)] hybrid is slowly lowered from ambient to 133 K, the absorbances at 406 and 422 nm increase smoothly as the Soret bands of both α(Zn) and β($Fe^{III}H_2O$) chromophores sharpen (Figure 3). In addition, the absorption maximum associated with the ZnP shifts slightly. The temperature dependence of the Soret band absorbance of the partner, [α($Fe^{III}H_2O$),β(Zn)] hybrid (Figure 4), is very different. The ZnP absorbance at 422 nm again increases smoothly upon cooling (Figure 4, Inset). However, this is *not* true for the absorbance associated with the Soret band of α($Fe^{III}(H_2O)$) within the hybrid. Instead, the relative absorbance at 406 nm increases

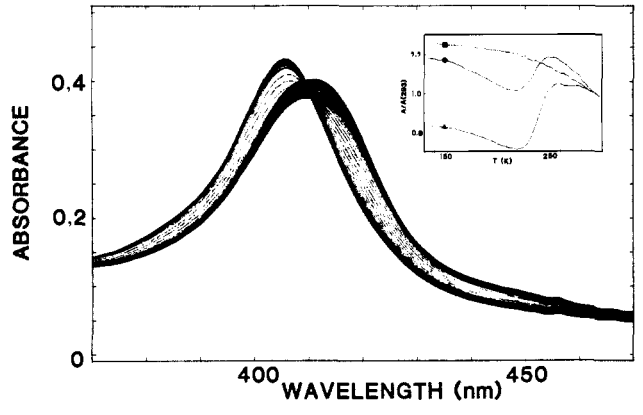

Figure 5. Temperature dependence of the optical spectrum α(Fe^{III}) subunits; T = 293–133 K (~3-deg increments). Inset: Absorbances normalized to the values at ambient temperature for α(Fe^{III}) subunits, λ = 406 nm (▲); metHb, λ = 406 nm (●); ZnHb, λ = 422 (■). Conditions: ethylene glycol/phosphate buffer cryosolvent; room temperature pH = 6.

(26) (a) McGlynn, S. P.; Azumi, T.; Kinoshita, M. *Molecular Spectometry of the Triplet State*; Prentice-Hall: Englewood Cliffs, NJ, 1969, pp 378–398. (b) Ratner, M., Northwestern University, personal communication.

as the sample is slowly cooled to ~ 250 K, but then decreases with further cooling until ~210 K, after which it again increases (Figure 5, inset). Thus, the chromophores in both chains of the [α(Zn),β($Fe^{III}H_2O$)] hybrid behave normally upon cooling, as does the ZnP in ZnHb (Figure 4, inset) and in the [α($Fe^{III}H_2O$),β(Zn)] hybrid. However, the α($Fe^{III}H_2O$) chain of the latter hybrid does not.

The temperature response of the optical spectrum of the [α-($Fe^{III}H_2O$),β(Zn)] hybrid indicates that the α(Fe^{III}) fully retains H_2O as the sixth ligand for $T \gtrsim 260$ K, that the ligation state of the α($Fe^{III}P$) changes as the temperature is slowly lowered through the range 260–210 K, and that the ligation state does not change further upon additional cooling. Two types of changes must be considered. Rifkind and co-workers[27] have shown that slow cooling of aquometHb leads to replacement of H_2O as the sixth heme ligand by the imidazole of the proximal histidine, thereby forming a bis(imidazole)ferriheme species called a hemichrome. Alternatively, because the pH of the cryosolvents increases as temperature decreases,[19] the spectra might be reflecting a change in the Hb ligand from H_2O to OH. The exact nature of the change within the hybrid has been ascertained by examining the temperature variation of the optical spectra of other Hb forms.

The isolated α($Fe^{III}H_2O$) and β($Fe^{III}H_2O$) subunits provide the simplest system to study. In both cases, the Soret band absorbance at 406 nm increases upon cooling from room temperature to ~280 K; over the next 50 deg, the 406-nm absorbance decreases and the maximum shifts to 412 nm; upon further cooling the absorbances at 406 and 412 nm again increase (Figure 5). The shift to 412 nm is equivalent to that observed upon addition of exogenous imidazole to aquomet-Hb,[28] demonstrating that the spectral change upon cooling is caused by coordination of the distal histidine to the ferriheme, as reported for metHb.[27] The intensity changes at 406 nm parallel those seen for the [α(Fe^{III}),β(Zn)] hybrid, indicating that both have the same origin. Within the hybrid, the shift in the Soret band of the α(Fe^{III}) chain is masked by the more intense absorbance of β(Zn).

The absorbance of aquometHb at 406 nm (Figure 5, inset) also varies with temperature in precisely the manner seen for the [α($Fe^{III}H_2O$),β(Zn)] hybrid (Figure 4) and for the isolated subunits (Figure 5). The shift in the Soret band of metHb is not so pronounced as in the isolated chains, indicating that only a fraction of the hemes form the hemichromes. Combining these several observations, we conclude that isolated subunits of both types form the hemichrome upon cooling, but for a tetrameric form of Hb, in particular for a [Zn,Fe^{III}] hybrid but apparently for aquometHb as well, the α($Fe^{III}H_2O$) chains undergo this transformation but the β($Fe^{III}H_2O$) chains do not.

EPR measurements confirm that hemichrome formation underlies the anomalous temperature variation in the optical spectra. In agreement with the results of Rifkind and co-workers,[27] metHb that had been slowly cooled to 175 K and then frozen to 77 K showed appreciable loss of the high-spin aquoferriheme signal seen in quench-frozen samples, as well as the appearance of the low-spin signal characteristic of bis(imidazole)ferriheme and associated with the internal hemichrome.

The possibility that α($Fe^{III}OH$) formation ($pK_a = 8$)[16] contributes to the spectral anomaly was examined by measuring the temperature dependence of the optical spectrum of metHb as a function of pH. Four samples were examined whose values for pH were 5.5, 6.0, 6.5, and 7.0 at room temperature and 6.5, 7.0, 7.5, and 8.0 at 190 K.[19] In all cases, the temperature variation of the optical spectra and the plots at the absorption of the Soret peak (406 nm) are similar and show the anomalous feature in the 200–250 K range, and the Soret maximum remains at ~406 nm upon cooling. The absence of any major change with pH appears to rule out a change in the protonation state of the α chain aquoferriheme as the source of the anomaly. Moreover, EPR

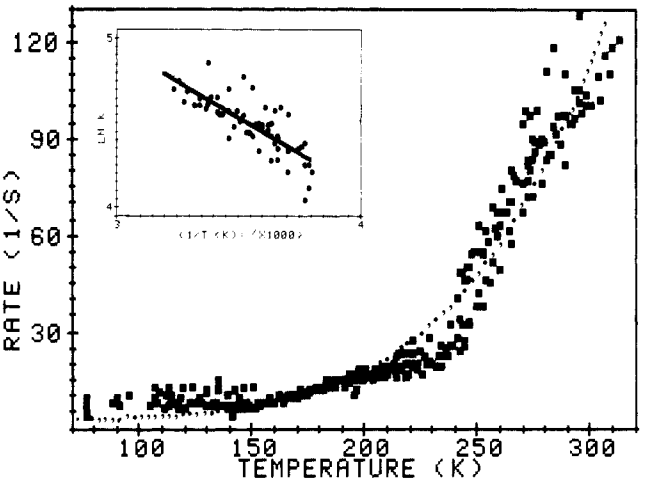

Figure 6. Temperature dependence of the electron-transfer rate, k_t, for [α(Zn),β($Fe^{III}H_2O$)] calculated from eq 3 as described in text. Curve represents fit of quantum-mechanical expression[12]; parameters listed in Table I. Inset: Arrhenius plot of the k_t in high-temperature regime; parameters listed in Table I.

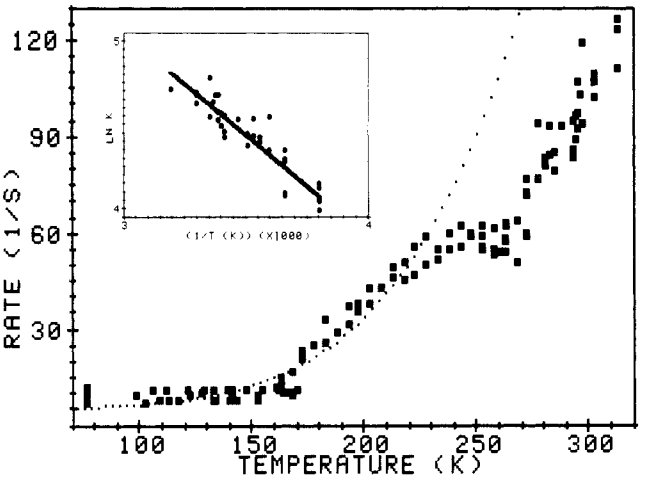

Figure 7. Temperature dependence of the electron-transfer rate, k_t, for [α(Fe^{III}),β(Zn)] calculated from eq 3 as described in text. Curve represents fit of quantum-mechanical expression[12] to data for $T \leq 230$ K because of change in heme ligation (see text); parameters listed in Table I. Inset: Arrhenius plot of the k_t in high-temperature regime; parameters listed in Table I.

spectra obtained at 4 K did not show significant amounts of hydroxyferriheme. However, an increase in the pH at ambient temperature appears to lower the onset temperature of the anomaly. In addition, we examined the temperature variation of the optical spectra of fluoro-, cyano-, hydroxo-, and (imidazole)metHb. Conversion to a hemichrome upon cooling should be suppressed when an exogenous ligand binds to the heme, and in each case the optical anomaly was abolished.

Temperature Dependence of k_t. The electron-transfer rate constants between 77 and 313 K for the two Hb hybrids were calculated according to eq 3 through use of the measured values of k_{obsd} and the analytic representation for k_D, eq 4. Use of the analytic expression for k_D allows for interpolation in the subtraction of eq 3; examination of the experimental data in Figures 1 and 2 shows that the procedure is fully justified. The results for the [α(Zn),β(Fe)] and [α(Fe),β(Zn)] hybrids are presented in Figures 6 and 7, respectively.

The electron-transfer rates for the two hybrids are the same at room temperature, and for each, k_t decreases rapidly upon cooling and becomes temperature-independent by $T \sim 140$–160 K, Figures 6 and 7 (or 1 and 2). Examination of the figures indicates the low-temperature tunneling rate constant to be ca. 5–10 s^{-1} for both hybrids. In order to obtain the best possible values for the low-temperature rate constants, numerous mea-

(27) (a) Levy, A.; Walker, J. C.; Rifkind, J. M. *J. Appl. Phys.* **1982**, *53*, 2066–2068. (b) Chukyniski, P. P.; Alston, K.; Rifkind, J. M., submitted for publication in *Biochem. Biophys. Res. Commun.* **1985**. (c) Levy, A.; Alston, K.; Rifkind, J. M. *J. Biomol. Struct. and Dyn.* **1984**, *1*, 1299–1309.

(28) Peisach, J.; Gersonde, K. *Biochemistry* **1977**, *16*, 2539–2545.

surements were made within the temperature range of 77–160 K on each of the four samples: [α(Zn),β(Fe^{II})], 45; [α(Zn),β(Fe^{III}H$_2$O)], 82; [α(Fe^{II}),β(Zn)], 28; [α(Fe^{III}),β(Zn)], 48. As seen in Figures 1 and 2, in the temperature-invariant range, the measurements of k_{obsd} for the [Zn,Fe^{III}] hybrids and k_D for the corresponding [Zn,Fe^{II}] hybrids do not overlap and their difference, k_t, although small, is well outside the scatter in the data. The electron-transfer rate constant for a hybrid in the temperature-invariant regime was calculated by two procedures: (1) The transfer rates plotted in Figures 6 and 7 were averaged over the low-temperature (77–160 K) range; for the [α(Zn), β(Fe^{III}H$_2$O)] hybrid $k_t = 8 \pm 2$ s^{-1} and for the [α(Fe^{III});β(Zn)] hybrid $k_t = 9 \pm 2$ s^{-1}. (2) The experimental values of k_{obsd} and of k_D for this range (Figures 1 and 2) were averaged; the difference of the averages (eq 3) gives $k_t = 8 \pm 2$ s^{-1} and $k_t = 10 \pm 3$ s^{-1} for the [α(Zn),β(Fe^{III}H$_2$O)] and the [α(Fe^{III}H$_2$O),β(Zn)] hybrids, respectively. The agreement between methods confirms that the tunneling rate constant is indeed well-defined by these experiments.

For the [α(Zn),β(Fe^{III}H$_2$O)] hybrid, the pronounced temperature dependence of k_t near ambient temperature changes to the temperature-independent behavior at low temperatures in a relatively smooth fashion (Figure 6). The temperature response of the optical spectrum of the [α(Zn),β(Fe^{III}H$_2$O)] hybrid shows that the ligation state of the ferriheme remains invariant upon cooling, and thus the values of k_t measured over the complete range of 77–313 K represent electron transfer from ^{3}ZnP to Fe^{III}(H$_2$O)P within the α_1–β_2 electron-transfer complex of tetrameric [α(Zn),β(Fe^{III}H$_2$O)] hybrid.

In contrast, the temperature response of k_t for the [α(Fe^{III}),β(Zn)] hybrid exhibits a plateau in the interval of about 230 to 270 K (Figure 7). The structure in the temperature response of k_t is not dependent upon the solvent, for it occurs well above the freezing point of each cryosolvent, ~190 K, and it is not observed for the complementary Hb hybrid [α(Zn),β(Fe^{III}H$_2$O)]. Because this feature is not observed in the temperature dependence of k_D but is manifest in k_{obsd} (Figure 2), it must indeed be a property of k_t. Figures 4 and 7 show that the anomaly in the temperature variation of k_t correlates with the formation of a hemichrome in the [α(Fe^{III}),β(Zn)] hybrid within the temperature interval of the anomaly. Thus, of the data set for the [α(Fe^{III}),β(Zn)] hybrid presented in Figure 7, the results for $T \gtrsim 260$ K represent electron transfer to ferrihemes that are fully in the form Fe^{III}(H$_2$O)P, whereas those for $T \lesssim 230$ K represent reduction of ferrihemes that to a large fraction have bound a distal histidine. The transition region, $230 \lesssim T \lesssim 270$, represents the gradual formation of the imidazole-bound form; the observation of a plateau implies that k_t increases upon formation of the hemichrome, but this is compensated by the decrease in k_t upon cooling.

In the high-temperature range, 260–313 K, where H$_2$O is bound to the ferriheme of both hybrids, the electron-transfer rate constants for the two are essentially equal. For a convenient comparison between the two species and for comparison with other work, k_t at high temperatures has been fit to the Arrhenius equation, $k_t = k_\infty \exp(E_{act}/RT)$ (Figures 6 and 7, insets), and the parameters are listed in Table I. The two hybrids behave quite similarly in the high-temperature range, consistent with visual inspection of Figures 6 and 7 (insets), but careful examination of the data does suggest that the differences between the two Hb hybrids, although small and not well established, may in fact be meaningful.

In the low-temperature region $k_t \sim 9$ s^{-1} for both hybrids. The similarity appears interesting because they have different ferriheme axial ligands in this temperature range, and the above analysis indicates that k_t for the imidazole-bound and H$_2$O-bound forms diverge as temperature increases. However, the low-temperature rates are small and the uncertainties could mask appreciable fractional differences. Moreover, the degree of ligand conversion in the [α(Fe^{III}),β(Zn)] hybrid has not been quantitated.

Theoretical Treatment of Electron Transfer. As a preliminary guide to future, more detailed, theoretical treatments of long-range electron transfer and as a means of summarizing our measurements for comparison with other studies, we have fit the electron-transfer rates for the [Zn,Fe] hybrids to expressions that describe nonadiabatic electron transfer involving vibronic coupling to a composite oscillator of a single frequency, ω, in both donor and acceptor. The simplest expression is that of Hopfield's semiclassical model;[29] derived from the Forster–Dexter theory of energy transfer, it represents an approximate solution to the problem of single-mode coupling and may be written in terms of three parameters[2a] (α, $T_c(\omega)$, and β):

$$k_t = \alpha_{sc}(\tanh(T_c/T))^{1/2} \exp(-\beta \tanh(T_c/T)) \quad (5)$$

Here, $\alpha_{sc} = (2\pi/\hbar)|H|^2/(2\pi\hbar\omega\lambda)^{1/2}$; H is the electron-tunneling matrix element; the reorganization energy, λ, is the energy required to alter the nuclear configuration from the equilibrium position on the reactant potential energy surface to the equilibrium position on the product potential energy surface in the absence of electron transfer. In the vicinity of the critical temperature, $T_c = \hbar\omega/2k_B$, the thermal energy becomes comparable to the vibrational spacings; as the temperature is raised through $T \sim T_c$, eq 5 predicts that the electron-transfer rate increases and becomes thermally activated. The third parameter is the ratio of the activation energy in the high-temperature, classical limit ($E^+ = (\Delta E_0' - \lambda)^2/4\lambda$, where $\Delta E_0'$ is the redox potential difference within the hybrid), to the vibrational energy: $\beta = E^+/k_BT_c$.

The exact quantum-mechanical description of the electron-transfer rate constant in the case of single-mode vibronic coupling also is available[12] and can be formulated in terms of three parameters,[2a] $\alpha_Q = 2\pi|H|^2/\hbar^2\omega$; $T_c = \hbar\omega/2k_B$; and $S = \lambda/\hbar\omega$,

$$k_t = \alpha_Q I_p(S/\sinh(T_c/T)) \exp[(pT_c/T) - S\coth(T_c/T)] \quad (6)$$

where I_p is the modified Bessel function and p is the ratio of the

Table I. Electron-Transfer Parameters in [Zn,Fe]Hb Hybrids at R(Zn–Fe) = 25 Å[a]

	[α(Zn),β-(Fe^{III}H$_2$O)]	[α(Fe^{III})β(Zn)][b]	*C. vinosum*[c]
$\Delta E_0'$, eV	~0.8[d]	ca. 0.7[b,d]	0.45
Arrhenius			
E_{act}, eV	0.074	0.11	0.18
k_∞, s^{-1}	1.9×10^3	6.0×10^3	7.8×10^8
quantum mechanical[e]			
α_Q, s^{-1}	2.4×10^5	1.6×10^5	1.14×10^{12}
S	42.4	37.0	43.9
$T_c(\bar{\nu})$[f], K	282 (392 cm^{-1})	281 (389 cm^{-1})	278 (386 cm^{-1})
λ, eV	2.06	1.79	2.10
E^+, eV	0.17	0.17	0.29
$\|H\|$, eV	1.1×10^{-6}	1.0×10^{-6}	2.4×10^{-3}
semiclassical[g]			
α_{sc}, s^{-1}	4.26×10^6	4.98×10^5	[h]
β	13.7	11.2	[h]
$T_c(\bar{\nu})$[f], K	299 (416 cm^{-1})	250 (347 cm^{-1})	206
E^+, eV	0.35	0.24	0.36
λ, eV	2.78	2.13	2.24
	(0.23)	(0.23)	(0.09)
$\|H\|$, eV	2.1×10^{-5}	3.8×10^{-6}	1.6×10^{-3}
	1.1×10^{-5}	6.4×10^{-6}	3.6×10^{-3}

[a] Edge-to-end distance ca. 20 Å. Parameters are defined in individual footnotes and in text. For the quantum-mechanical and semiclassical theories, the first three parameters are the result of the fitting procedures and the others are calculated from them. [b] As described in the text, the parameters refer to a hydrid in which the majority of the α-hemes may be described as α(Fe^{III}Im), where the distal histidine is bonded to iron. [c] Data from ref 2a. [d] Ref 11. The value of |α(Fe^{III}),Zn] relies on the approximation that imidazole binding changes the ferriheme reduction potential as does azide binding (ref 11c). [e] Equation 5, theory of ref 12: $\alpha_Q = 2\pi|H|^2/\hbar\omega$; $T_c = \hbar\omega/2k_B$; $S = \lambda/\hbar\omega$; $E^+ = (\Delta E_0' - \lambda)^2/4\lambda$. [f] $\bar{\nu} = 2k_BT_c/hc$. [g] Equation 6, theory of ref 29: $\alpha_{sc} = (2\pi/\hbar)|H|^2/(2\pi\hbar\omega\lambda)^{1/2}$; $\beta = E^+/k_BT_c$; $T_c = \bar{\omega}/2k_B$. [h] Not given in ref 2, but calculable from equations in text and other parameters.

(29) See (a) Debrunner, P. G.; Frauenfelder, H. *Annu. Rev. Phys. Chem.* **1982**, *33*, 283–299. (b) Petsko, G. A.; Ringe, D. *Annu. Rev. Biophys. Bioeng.* **1984**, *13*, 331–371 and references therein.

exoergicity ($\Delta E_0'$) to the vibrational spacing ($\hbar\omega$).

[α(Zn),β(Fe^{III}(H$_2$O)]. The variation of k_t for this hybrid over the range 77–313 K presented in Figure 6 can be well fit both by the semiclassical (eq 5) and quantum-mechanical expressions[12] for $k_t(T)$; the parameters to these expressions are listed in Table I. The quantum-mechanical curve is presented in Figure 6, and only the parameters from this treatment will be discussed. To the extent that theory differs from experiment, the theoretical curves show a more gradual transition from the temperature-independent to the strongly temperature-dependent regimes, but the spread in the experimental measurements and examination of individual experiments leads us to believe that this apparent abruptness is not significant. In either case, the apparent onset of a stronger temperature variation in k_t at ca. 240 K does not signify a change in the state of the protein. This temperature does not correspond to the freezing point of the solvent ($T \cong 190$ K), and the optical spectrum shows no unusual behavior at the ferriheme near 240 K, and in particular rules out hemichrome formation.

In the theoretical expressions, k_t ceases to be temperature-independent and becomes thermally activated as the temperature is increased through the critical temperature ($T_c = 282$ K). This temperature corresponds to a vibrational frequency for the composite oscillator that is consistent with those observed for metal–ligand vibrations. The classical, high-temperature energy of activation calculated from the quantum-mechanical parameters (Table I) is 2–3 times greater than that calculated from the Arrhenius equation. This is because the data used to fit the Arrhenius equation was obtained in the vicinity of T_c (263 K < T < 313 K) and therefore is not representative of the high-temperature classical regime. Interestingly, the single-mode theory predicts that for $T > T_c$ the rate constant increases exponentially, but it appears that the experimental data for the [α(Zn),β-(Fe^{III}H$_2$O)] hybrid may be leveling off at $T > 290$ K (Figure 6). If this discrepancy can be verified, it would correspond to a limitation of the single-mode treatment; for example, it might represent the effects of anharmonicity.

The reorganization energy, λ, can be compared with the reorganizational enthalpies, ΔH^* ($\approx\lambda/4$),[2b,d] for electron transfer within ruthenium-modified cytochrome *c* and myoglobin. Oxidation of ZnP within the α(Zn) chain should be accompanied by minimal structural changes, and we may estimate the attendant reorganization energy, λ_{Zn}, to be no larger than that for oxidation of the heme of cytochrome *c*, $\lambda_{Zn} \lesssim \lambda_c \approx 4\Delta H_c^* \lesssim 1.2$ eV (~ 28 kcal mol^{-1}).[3d] In contrast, reduction of an aquoferriheme is accompanied by loss of the coordinated H$_2$O, motion of the iron with respect to the porphyrin mean plane, and changes in the porphyrin geometry. The reorganization energy for the heme in the β-(Fe^{III}H$_2$O) chain of the hybrid can be equated to that for the heme of myoglobin ($\Delta H_{Mb}^* \approx 20$ kcal mol^{-1};[3i] $\lambda_{Fe} \approx \lambda_{Mb} \approx 4\Delta H_{Mb}^* \approx 3.5$ eV. If the two centers within the $\alpha_1\beta_2$ complex behave independently, then[2b,d] one calculates $\lambda_{calcd} = (\lambda_{Zn} + \lambda_{Fe})/2 \lesssim 2.3$ eV, in good agreement with the experimental value, $\lambda \approx 2.1$ eV (Table I).

This agreement suggests that no major component of the reorganizational energy is associated with interactions at the interface between the subunits comprising the tightly bound $\alpha_1\beta_2$ complex. It will be interesting to see whether the same is true in the physiological complex between cytochrome *c* peroxidase and cytochrome *c*.[6] Also, it will be important to explore whether the reorganization associated with the ferriheme reduction is coupled to large-scale conformational fluctuations,[29] and not merely to localized vibrations, since motion of the iron with respect to the heme plane can cause a coupled motion of a portion of the F-helix of that chain.[10] Indeed, the existence of such conformational modes might serve to distinguish electron transfer in proteins from that in small molecules.

[α(Fe^{III}),β(Zn)]. To parameterize the theoretical models, data are necessary both in the high-temperature range, where k_t varies with T, and in the low-temperature tunneling regime, where k_t is essentially invariant. Because the [(Fe^{III}H$_2$O),β(Zn)] hybrid undergoes replacement of the ferriheme axial ligand, H$_2$O → Im, in the vicinity of 250 K, we have employed the measurements from 77 to 230 K as representing the properties of a single hybrid form, [α(Fe^{III}Im),β(Zn)], and have fit them with the semiclassical and quantum-mechanical expressions; the quantum-mechanical curve is displayed in Figure 7. The resulting parameters given in Table I are mainly of heuristic value because of uncertainty about the degree of ligand conversion and because of the limited data in the range where k_t varies with temperature. Nevertheless, the theoretical expressions predict a room-temperature electron-transfer rate constant of 160 s^{-1}, in good agreement with a preliminary measurement of $k_t = 170$ s^{-1} for a hybrid with exogenous imidazole bound to the ferriheme.

From Table I it appears that the major difference between electron transfer to the high-spin Fe^{III}(H$_2$O)P and to the low-spin Fe^{III}(Im)P of the hemichrome is a lower reorganization energy for the latter. Although such a difference normally is expected when a low-spin heme remains six-coordinate upon reduction,[2,3h,i] it is of particular interest in this instance, since both H$_2$O and exogenous Im are believed to dissociate upon reduction of the ferriheme. Indeed, the decrease in λ may have contributions that are as "simple" in origin as the larger size of imidazole compared to H$_2$O. The increased size of a redox center having imidazole coordinated to the heme would lower the contribution to the "outer-sphere" reorganization energy from polarization of the protein medium acting as the "solvent" for the center.[2d] Clearly, the electron-transfer parameters for [α(Fe^{III}Im),β(Zn)] must be remeasured with samples prepared by using exogenous imidazole and related ligands.

For comparison purposes only, we also have fit the high-temperature data ($T > 260$ K) as representing the [α(Fe^{III}H$_2$O)β(Zn)] hybrid, using $k_t = 9$ s^{-1} as the low-temperature tunneling rate. The resulting parameters are not listed, but agree well with those for the [α(Zn),β(Fe^{III}H$_2$O)] hybrid.

Discussion

This report presents the first full temperature response of long-range electron transfer in a system of known architecture, the complementary [Zn,Fe^{III}]Hb hybrids. For both hybrids k_t exhibits a thermally activated regime in which nonadiabatic electron transfer is coupled to thermal vibrations and fluctuations within the α_1–β_2 electron-transfer complex and its environment. Below ca. 140–160 K the fluctuations that induce electron transfer "freeze out"; k_t for the hybrids becomes independent of temperature, and the transfer process involves nonadiabatic electron tunneling in which the accompanying nuclear rearrangement proceeds by nuclear tunneling. The transition between these two regimes differs dramatically in the two hybrids because of different responses of the Fe^{III}P coordination state to cooling. Optical and EPR measurements show that the heme of the [α(Fe^{III}H$_2$O),β-(Zn)] species forms a hemichrome upon cooling, but the [α-(Zn),β(Fe^{III}H$_2$O)] hybrid remains invariant.

How do the present results compare with those for long-range electron transfer in other protein systems? The analyses of the temperature variation of k_t for the hybrids have been compared above with those for experiments in the range $T \gtrsim 0$ °C with ruthenium-modified proteins. Because the full temperature response of the k_t for the [α(Zn),β(Fe^{III}H$_i$O)] hybrid has been measured and analyzed within the quantum-mechanical theory, it seems particularly interesting to compare the electron-tunneling process in the hybrid with that in the first system so characterized, the photosynthetic reaction center of *C. vinosum*.[13] In the latter case a cytochrome ferroheme is oxidized by a radical that is associated with a bacteriochlorophyll (BChl-b) special pair. The

$$Fe^{II}P + (BChl\text{-}b)_2^+ \rightarrow Fe^{III}P + (BChl\text{-}b)_2$$

photosynthetic reaction is much more rapid than electron transfer from ^{3}ZnP to Fe^{III}(H$_2$O)P in the α_1–β_2 complex. For example, the electron-transfer rate in the former system is ca. 10^4 times larger at ambient temperature and ca. $10^{1.5}$ times greater in the low-temperature tunneling regime. Thus, both the scale of the transfer rates, determined at low temperatures, and the temperature responses differ.

What is the basis of these differences? The quantum-mechanical parameters in Table I suggest that it does *not* reflect differences in vibronic coupling. The two systems have essentially the same critical temperatures and reorganization energies, indicating that the frequency of the coupled composite oscillator and the extent of nuclear reorganization upon electron transfer are comparable in the photosynthetic system and in the hemoglobin hybrids. The difference in temperature dependences is associated with the difference in exothermicity for the two reactions; the classical, high-temperature activation energy, $E^{\dagger}$, for *C. vinosum* is ca. 1.5 that for the hybrid. The scale of the rates is set by the electron-transfer matrix element, H, which is much greater for the photosynthetic system: $H(C.\ vinosum)/H(\text{hybrid}) \sim 2 \times 10^3$. This large ratio of matrix elements would suggest either that the redox partners in *C. vinosum* are substantially closer than in the hybrids or that the influence of orientation and/or the protein medium facilitates electron transfer in the photosynthetic system: the structure of the reaction center of *R. viridis* supports the latter, more interesting, possibility.[30]

Acknowledgment. We acknowledge Dr. D. Gingrich and M. Y. Ogawa for assistance in the EPR measurements, and Drs. J. Rifkind, H. B. Gray, M. Ratner, N. Sutin, M. Newton, J. R. Miller, and J. Peisach for helpful discussions. We thank Dr. Rifkind for communication of unpublished results. This work has been supported by the National Institutes of Health (HL 13531) and the National Science Foundation (PCM 8305218).

Registry No. ZnP, 15442-64-5; $Fe^{III}P$, 16009-13-5.

(30) Deisenhofer, J.; Epp, O.; Miki, K.; Huber, R.; Michel, H. *J. Mol. Biol.* **1984**, *180*, 385-398.

Molecular Motions of Alkoxysilanes Immobilized on Silica Surfaces: A Deuterium NMR Study

Eric C. Kelusky[†] and Colin A. Fyfe*

Contribution from the Guelph-Waterloo Center for Graduate Work in Chemistry, Guelph Campus, Department of Chemistry and Biochemistry, University of Guelph, Ontario, Canada N1G 2W1. *Received December 26, 1984*

Abstract: The motional dynamics of surface-attached chains have been studied by ^2H NMR. Deuterated alkoxysilanes were immobilized on silica gel and investigated both in the solid state and in the presence of solvents. In the solid state, the spectra exhibit motionally narrowed line shapes with the greatest narrowing and therefore the most motion being observed for the longest chains. The motions in the solid state persist to temperatures as low as 150 K and are likely isotropic in nature. Hexane and benzene have only a limited effect on the mobility of the alkoxysilanes. Methanol is able to solubilize a portion of the alkoxysilanes, but at least half of the chains are unaffected by the addition of methanol.

In the last several years there has been considerable growth in interest in the study of surface-modified silicas. These studies have been greatly facilitated by the application of magic angle spinning[1] and cross polarization[2] techniques to obtain high-resolution ^{13}C and ^{29}Si spectra of surface-immobilized species.[3-6] While these techniques allow substantial characterization of the surface, they do not give information on the nature of the motions which occur. Motional dynamics of surface-modified silicas have been probed by ^{13}C relaxation measurements,[7] and static ^{13}C chemical shift anisotropy patterns have given useful information on the molecular motions of surface-immobilized phenyl groups.[8] However, acquisition of this type of data is time-consuming and the results are open to some interpretation.

As an alternative approach, it is also possible to probe molecular motions by wide-line ^2H NMR. This technique has several advantages for studies of molecular motion: Since the quadrupole interaction, which dominates the spectra, is essentially axially symmetric, the spectral line shapes are simple and dependent upon the amplitude and symmetry of the molecular motions. As well, by synthetic incorporation of deuterium, the technique is sensitive and usually much less expensive than a comparable incorporation of a ^{13}C label. In addition, the technique is completely nonperturbing. Studies of molecular motion by ^2H NMR have, to date, been essentially limited to biological membranes[9] and some polymers,[10] but they have yielded incisive results in these areas.

In order to probe the molecular motions occurring on surfaces, we have undertaken a ^2H NMR study of several deuterium-containing alkoxysilanes, chemically bonded to silica. The surface-immobilized alkoxysilanes, which contained completely deuterated alkoxy groups and ranged from one carbon to sixteen carbons in length, are shown in Figure 1. The motional behavior of these surface-modified silicas has been probed in the solid state. As well, since these compounds are models for chromatographic materials, the influence of various solvents on the mobility of the alkoxy groups has also been studied.

Experimental Section

Dimethyldichlorosilane was obtained from Petrarch Systems Inc. (Levitown, PA) and the deuterated alcohols were purchased from MSD Isotopes, Montreal, Canada. Fisher S-157 silica gel (28-200 mesh) was predried by heating to 200 °C on a vacuum line.

The deuterated silating reagents were prepared by slowly adding a deuterated alcohol (30 mmol) to dichlorodimethylsilane (28 mmole) with the reaction mixture maintained at 0 °C. The resulting product, which

[†] Present Address: DuPont Canada Inc., Research Centre, Box 5000, Kingston, Ontario, Canada K7L 5A5.

(1) Andrew, E. R. *Prog. Nucl. Magn. Reson. Spectrosc.* **1971**, *8*, 1-79.
(2) Pines, A.; Gibby, M. G.; Waugh, J. s. *J. Chem. Phys.* **1973**, *59*, 569-589.
(3) Maciel, G. E.; Sindorf, D. W.; Bartuska, V. J. *J. Chromatogr.* **1981**, *205*, 438-443.
(4) Hays, G. R.; Clague, A. D. H.; Huis, R. *Appl. Surf. Sci.* **1982**, *10*, 247-263.
(5) Sindorf, D. W.; Maciel, G. E. *J. Phys. Chem.* **1982**, *86*, 5208.
(6) Sindorf, D. W.; Maciel, G. E. *J. Am. Chem. Soc.* **1983**, *105*, 3767-3776.
(7) Sindorf, D. W.; Maciel, G. E. *J. Am. Chem. Soc.* **1983**, *105*, 1848-1851.
(8) Slotfeldt-Ellingsen, D.; Resing, H. A. *J. Phys. Chem.* **1980**, *84*, 2204-2209.
(9) Davis, J. H. *Biochim. Biophys. Acta* **1983**, *737*, 117-171.
(10) Spiess, H. W. *Colloid Polym. Sci.* **1983**, *261*, 193-209.

0002-7863/86/1508-1746$01.50/0